



CAD-to-Print Strategy for Gas Metal Arc Directed Energy Deposition

ORCID: Birendra Kumar Barik: <https://orcid.org/0000-0001-9517-8335>
ORCID: Prashant Kumar Chaurasia: <https://orcid.org/0000-0002-5857-6833>
ORCID: Amitava De: <https://orcid.org/0000-0002-3109-261X>

Birendra Kumar Barik^{*,1}, Prashant Kumar Chaurasia², Amitava De³

^{1,2,3}Mechanical Engineering Department,
Indian Institute of Technology Bombay, Mumbai- 400076, India

¹Production Engineering Department,
Veer Surendra Sai University of Technology Burla, Odisha- 768018, India
Email: ¹birenbarik_pe@vssut.ac.in, ²prashant9161@gmail.com, ³amit@iitb.ac.in

*Corresponding author

DOI : 10.22486/iwj.v57i2.43850

Abstract

Harnessing between a computer-aided design (CAD) and the actual printing of a part is by far the most arduous task for robotic gas metal arc directed energy deposition (GMA-DED). The generation of a suitable scanning strategy to deposit overlapping tracks and successive layers is currently not supported by an organized single source. Three easy-to-use CAD-to-Print approaches— point-based, feature-based and drawing-based— are presented here utilizing the open-source software for robotic GMA-DED. The point-based approach involves the discretization of the CAD model into a set of target points and suitable for linear paths and regular geometry. The feature-based approach involves the generation of the robot scan path by slicing of the CAD model. It can consider both regular and irregular geometries but suitable for linear paths only. The drawing-based approach involves the robot scan paths drawn along the contours of the CAD model and is flexible for both linear and non-linear scanning paths. Although all the three approaches require user intervention, they have the potential for automation.

Keywords: Wire Arc Additive Manufacturing; Gas Metal Arc Directed Energy Deposition (GMA-DED); CAD-to-Print; Path Planning; Offline Robot Programming.

1.0 INTRODUCTION

Gas metal arc directed energy deposition (GMA-DED) is the most important technology among various wire arc additive manufacturing (WAAM) processes. GMA-DED involves the fabrication of a part from its computer-aided design (CAD) model and requires the selection of suitable process parameters and an efficient path planning for the welding torch [1-3]. Currently, the welding torch in robotic GMA-DED requires the use of a teach pendant and several iterations to arrive at a suitable scan path, which is tedious and time-consuming [4-6]. As the interest on WAAM is growing in several user industries, there is a substantive demand for an easy-to-use and reproducible methodology for the path planning of the welding torch in robotic GMA-DED [7]. In

particular, easy-to-use unified digital tools, which can provide a suitable scanning strategy for the printing of a 3D metallic part directly from its CAD file, are needed but currently scarce [8-9].

The CAD-to-Print strategy broadly encompasses three stages: (a) slicing of part geometry, (b) path planning for the welding torch, and (c) robot code generation [4]. Although dedicated software solutions are available for the first step, similar tools that can provide a seamless solution for all the three required steps are yet unavailable. Substantial efforts are reported in the recent literature to develop CAD-to-Print capability for GMA-DED [8-13]. Ding et al. [8] used machine learning techniques for the development of a suitable scanning strategy of the welding torch. A modular path planning was presented by Michel et al. [10] by segmenting the CAD model into distinct

zones and considering different process conditions such as wire feed rate (WFR) and printing travel speed (PTS) for different zones. A continuous path planning for the welding torch from the bottom to the top layers was employed following the CAD model to reduce the multiple arc start and stop [9,11]. Diourte et al. targeted a path planning strategy to ensure the welding torch to remain perpendicular to the deposition plane [8]. Giordano et al. [11] developed a continuous spiral path planning strategy from substrate to upper layers based on numerically computed temperature field. However, dimensional inconsistency and distortion due to heat accumulation along the part height was a major challenge. Chernovol et al. [12] used a commercial CAD software to construct the scanning strategy for a thin wall deposition, which did not allow much customization. Onstein et al. [13] used a robot specific software to generate the robot scan path based on the point cloud on the CAD model surface. The aforementioned investigations pointed out a growing interest to realise a CAD-to-Print capability for GMA-DED using various commercial and open-source software. An efficient and easy-to-use approach for path planning and robot program generation using open-source software is still in demand.

The finding of the scan path for the welding torch in GMA-DED requires a prior knowledge of the part geometry, track and layer dimensions, and the important process conditions such as WFR and PTS [14-15]. The part geometry is described by a CAD model, which is required to be sliced into segments for multi-directional deposition using a filler wire [16-17]. The generation of such slices requires a prior knowledge of the track and layer profiles that are to be deposited [15]. It is

imperative that suitable process conditions to deposit the target track and layer profiles are known. The robot code for the movement of the welding torch must be generated and tested before the actual deposition begins. A robot specific software [18] and an open source CAD software [19] are used in the present work and they are harnessed through a Python script to develop and demonstrate three CAD-to-Print approaches in the present work.

2.0 METHODOLOGY

Three CAD-to-Print approaches- (a) point-based, (b) feature-based, and (c) drawing-based- are presented in this work. The steps for each of these approaches, and their respective working principles, advantages and limitations are presented in this section.

The point-based and drawing-based approaches use the vertex and contour information of the CAD model, respectively. In contrast, the edges of a sliced CAD model are used as a feature to generate the path in case of the feature-based approach. The resulting scanning strategy from these three approaches is fed as the teach pendant program (TPP) that finally controls the actual robot. The suitable process conditions such as WFR and PTS are included in the TPP. A prior knowledge of the width (w) and height (h) of the single-track deposit for different combinations of WFR and PTS are required to decide the suitable hatch spacing (δ) and path planning. The hatch spacing (δ) is defined as the centre distance between the two adjacent overlapped tracks [20].

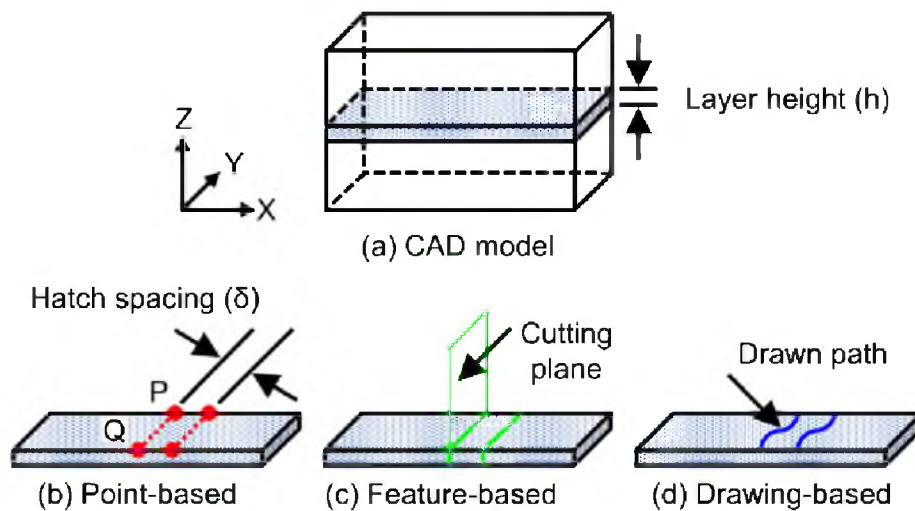


Fig. 1: (a) Geometric CAD model of target feature, and three different approaches; (b) point-based, (c) feature-based, and (d) drawing-based for the CAD-to-Print.

Fig. 1 (a-d) schematically show a CAD model of a target and three different CAD-to-Print approaches. A strip of thickness equal to the layer height (h) is considered as shown in **Fig. 1(a)**, where the layer height is equal to the height of a single-track. The tool centre point (TCP) is taken at the tip of the filler wire, which is moved from an arbitrary point P to a point Q to trace a designated path. **Fig. 1(b)** shows schematically the point-based approach where the TCP coordinates are obtained by discretising the CAD model using a Python script. In feature-based approach (**Fig. 1(c)**), the paths are generated through several vertical and horizontal cutting planes using an open source CAD software. For example, the feature in **Fig. 1(c)** is created by vertical slices of a horizontal layer. In the case of a drawing-based approach shown in **Fig. 1(d)**, the appropriate paths are drawn on a CAD model. The target points, sliced edges, and the drawn paths corresponding to the point-, feature-, drawing-based approaches are imported into the robot specific software to generate the TPP. A further detailed description of each approach along with the flow-chart is provided in the following sections.

2.1. Point-based approach

The point-based approach considers the coordinate positions of the vertices within a CAD model. This approach assumes that the CAD model possesses a regular and simple shape, and the deposition of the tracks and layers will maintain consistent profiles. The start and the end instructions for the welding torch for different layers are inserted separately. Following algorithm outlines the steps involved for the point-based approach.

Step 1. Input parameters

- Dimension of the CAD model: length (L), breadth (B), and height (H)
- Suitable process parameter: PTS and WFR
- Single track dimension: track width (w) and layer height (h)

Step 2. Input hatch spacing (δ)

Step 3. To determine number of layers (n_l) and tracks (n_t)

- $n_l = (H/h)$
- $n_t = (L/\delta)$

Step 4. To discretize each layer into points

- Start point: $S(x_{sr}, y_{sr}, z_s)$
- Discretized points:
 $P [x_{sr} + (i-1) \delta, y_s + B, z_s], Q [x_{sr} + (i-1) \delta, y_{sr}, z_s]$
 where $i = 1, 2, 3 \dots n_t$

Step 5. To register points into tool centre point (TCP)

- Convert the Cartesian coordinate (x, y, z) of each point into TCP (x, y, z, w, p, r), where w, p and r

are rotational angles about the x -, y -, and z -axes, respectively.

Step 6. To import registered points into the robot specific software

- Target points act as the path

Step 7. To generate robot program

- Robot code generation with suitable process parameters WFR and PTS

Step 8. To simulate virtual deposition

- Virtual deposition simulation to ensure correctness of the robot path program

Step 9. Output teach pendant program (TPP)

- Virtual Transfer TPP to teach pendant for dry run before final execution

Fig. 2 shows the flowchart of the point-based approach, which is constructed based on the aforementioned algorithm.

In summary, the point-based approach offers notable advantages including simplified path programming and expedited generation of robot code. The utilization of a generalized Python code for discretizing CAD models adds another layer of flexibility, enabling a seamless adaptation to changes in input parameters. However, this method is constrained to the fabrication of simple and regular shapes. It is tedious and often extremely difficult to find out the coordinate of the starting point for each layer for curvilinear geometry. The number of points also increases for non-linear paths leading to a higher volume of lines in the robot program. In turn, the robotic system is constrained by teach pendant memory limitations. For parts with either regular or irregular shapes, the feature-based approach offers a more suitable solution, as elaborated in the subsequent section

2.2. Feature-based approach

The initial assumptions regarding single-track deposition parameters, the number of tracks, the number of layers, and hatch spacing calculations in the feature-based approach align with those in the point-based approach. However, the feature-based approach provides a capability to generate linear track paths for both regular and irregular shapes with a greater ease. It involves the definition of cutting planes for horizontally slicing the CAD model based on the layer height, and for each sliced layer, cutting planes are established in the vertical direction, considering the hatch spacing. The start and the end points of the welding torch are specified at the corners of each horizontally sliced layer, which is changeable for different layers. Following algorithm outlines the steps involved for the development of a scanning strategy using feature-based approach.

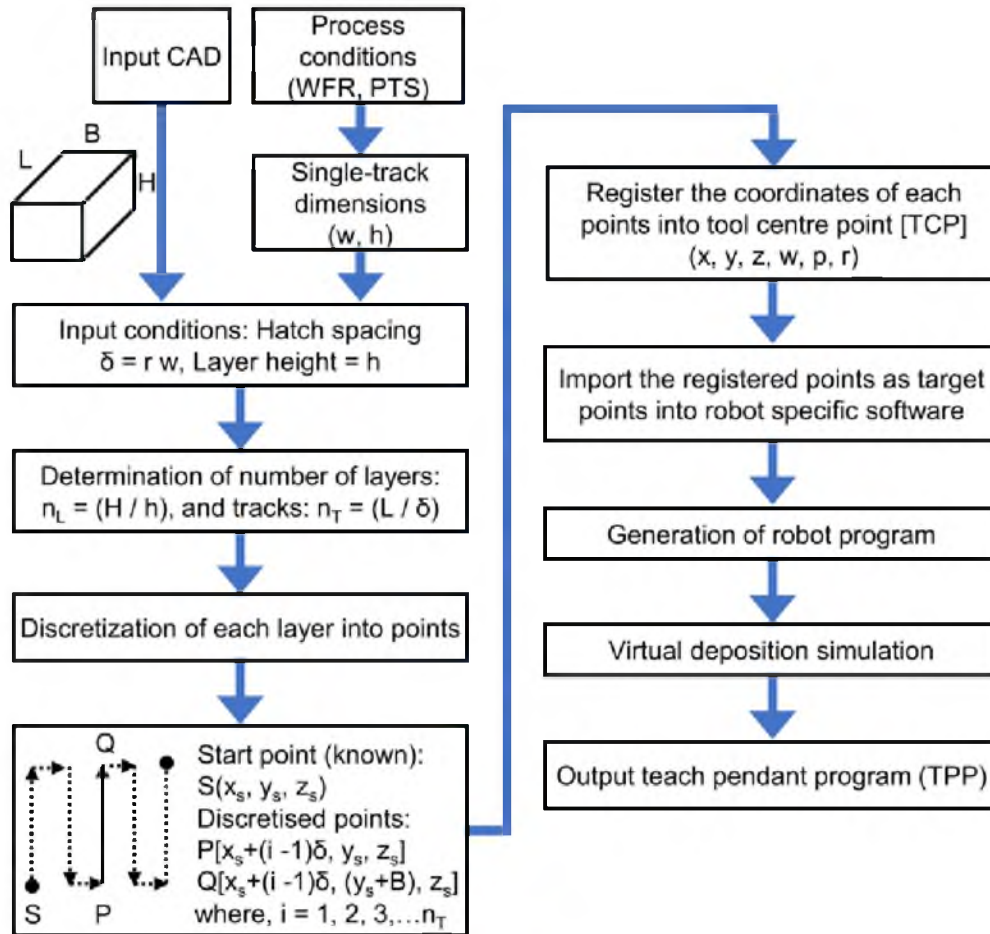


Fig. 2 : Flow chart of the point-based approach

Step 1. Input parameters

- Dimension of the CAD model: length (L), breadth (B), and height (H)
- Suitable process parameter: PTS and WFR
- Single track deposit dimension: track width (w) and layer height (h)

Step 2. Input hatch spacing (δ)

Step 3. To slice the CAD model to layers with horizontal cutting planes

- Horizontal cutting planes: $z = i * h; i = 1, 2, 3... (n_L - 1)$, where $n_L = (H/h)$

Step 4. To slice each layer with vertical cutting planes

- Horizontal cutting planes: $x = j * δ; j = 1, 2, 3... (n_T - 1)$, where $n_T = (L/δ)$

Step 5. To import sliced CAD model into the robot specific software

- Layer-wise importing is necessary to accommodate varying arc start and end locations for different layers.

Step 6. To create feature along the cutting edges

- Path planning using the feature based on the scanning strategy

Step 7. To generate robot program

- Robot code generation with suitable process parameters WFR and PTS

Step 8. To simulate virtual deposition

- Virtual deposition simulation to ensure correctness of the robot path program

Step 9. Output teach pendant program (TPP)

- Transfer the TPP into teach pendant for the dry run before final execution

Fig. 3 shows the flowchart of the feature-based approach, which is constructed based on the aforementioned algorithm.

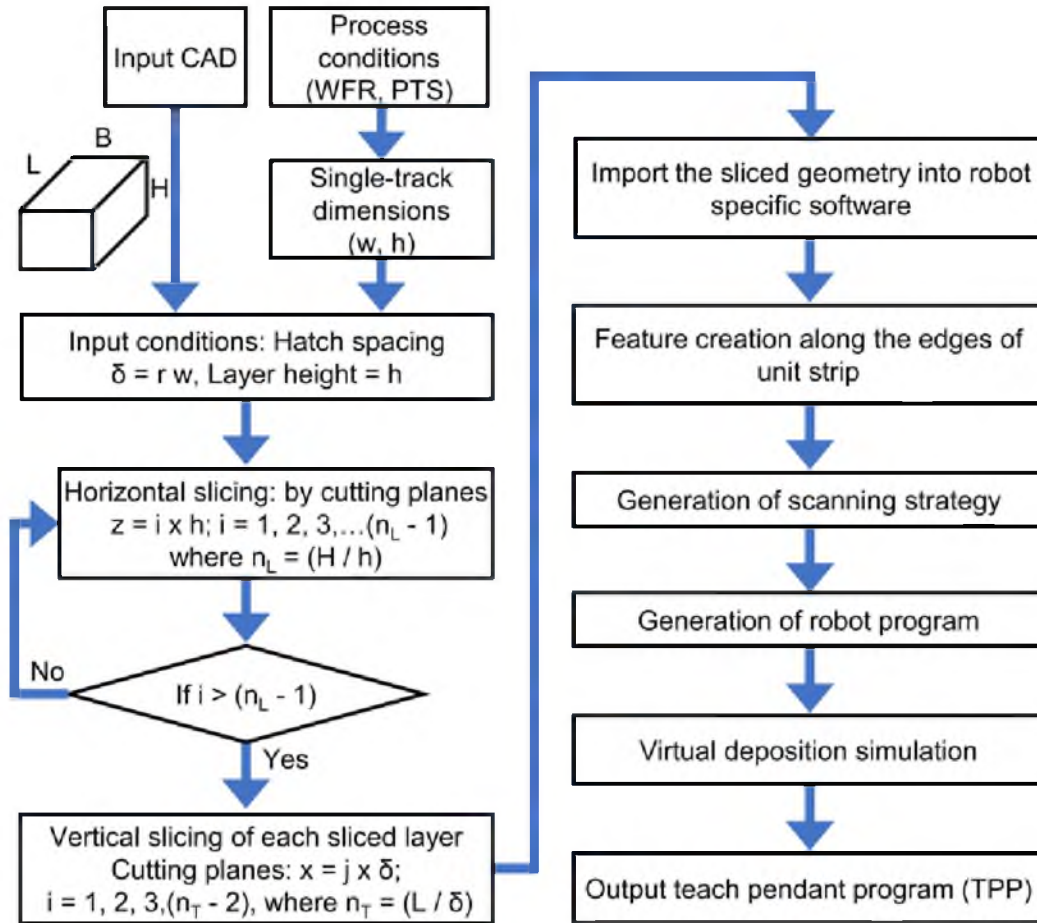


Fig. 3 : Flow chart of the feature-based approach.

The sliced CAD geometry in IGES (Initial Graphics Exchange Specification) format needs to be exported in robot specific software. This format ensures that cutting edges are easily detected, simplifying the process of feature creation. The mathematical concept of the cutting plane is given in the Appendix-I. The benefits of this approach lie in its ability to offer tailored path planning for parts of regular and irregular shapes. Adaptive layer height can be possible by considering of suitable cutting planes during horizontal slicing. However, it's important to note that in irregular shapes, aligning the non-linear path with the deposition path can result in multiple arc start and end points during the deposition process. This can adversely affect dimensional consistency.

2.3. Drawing-based approach

The drawing-based approach offers the flexibility to employ non-linear scanning strategies. This approach assumes that the contour of the part to be deposited can be drawn directly

onto the CAD model of the substrate. The contour of the horizontally sliced CAD model of the deposition part is necessary to accommodate varying arc start and end points for each layer. Following algorithm outlines the steps involved for the development of a scanning strategy using drawing-based approach.

Step 1. Input parameters

- Dimension of the CAD model: length (L), breadth (B), and height (H)
- Suitable process parameter: PTS and WFR
- Single track deposit dimension: track width (w) and layer height (h)

Step 2. Input hatch spacing (δ)

Step 3. To determine number of layers (n_L) and tracks (n_T)

- n_L = (H/h)
- n_T = (L/δ)

Step 4. To draw path along the contour of the CAD model

- Tracks to be drawn on the surface of substrate

Step 5. To import drawn feature into the robot specific software

- Layer-wise drawing is necessary to accommodate varying arc start and end locations for different layers.

Step 6. To generate robotic tool path along the drawn feature

- Path planning using drawn feature based on the scanning strategy

Step 7. To generate robot program

- Robot code generation with suitable process parameters WFR and PTS

Step 8. To simulate virtual deposition

- Virtual deposition simulation to ensure correctness of the robot path program

Step 9. Output teach pendant program (TPP)

- Transfer the TPP into teach pendant for the dry run before execution

Fig. 4 shows the flowchart of the drawing-based approach based on the aforementioned algorithm that assumes the non-linearity of the CAD model along the deposition direction only. For the regular shape, the depositing paths are drawn on the substrate only once, which is given by an offset for successive layers further. In contrast, the depositing paths are drawn for each layer for the irregular shape along the build height.

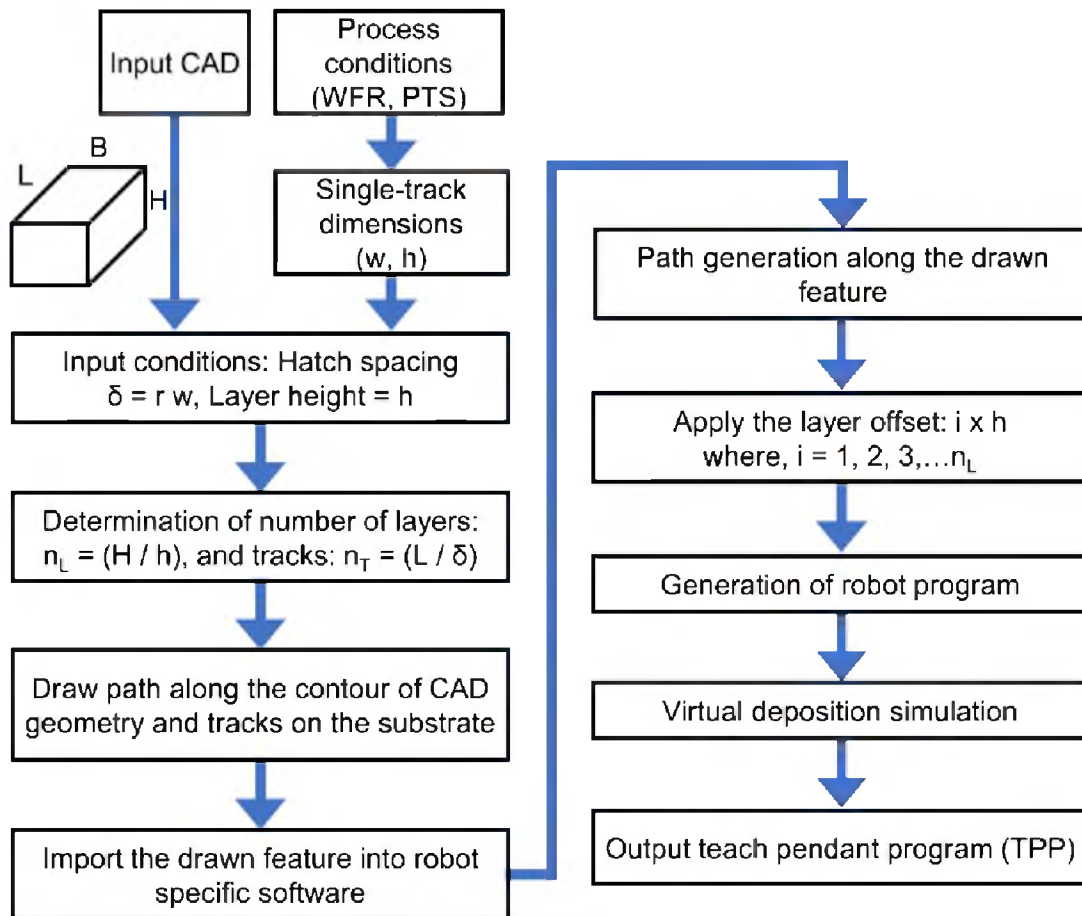


Fig. 4 : Flow chart of the drawing-based approach

The merits of this approach lie in its ability to perform path planning based on drawn features and its versatility in accommodating both linear and non-linear track configurations. It is particularly well-suited for regular shapes and offers manual operation with the potential for automation. However, while this approach excels in handling non-linear tracks, its superiority over the feature-based approach is depends upon the orientation of the deposition part.

3.0 RESULTS AND DISCUSSION

The relative efficacy of the three proposed CAD-to-Print approaches is evaluated for a single-track multi-layer thin linear wall and multi-track multi-layer non-linear build deposition based on the computational time, complexity of the robot program, software involvement, and user intervention.

3.1. Single-track multi-layer linear wall

Fig. 5(a-c) show the generated scanning strategy for the single-track five-layer wall using the point-based, feature-based and drawing-based approaches, respectively. Given a CAD model with dimensions of 100 mm (length), 10 mm (height), and 5 mm (width), and considering a track length of 100 mm, a layer height of 2 mm, and width of 5 mm, there are 5 layers and 1 track in total. A bidirectional scanning strategy is considered that usually results in an improved dimensional consistency [21].

Fig. 5(a) shows the robot scan path following point-based approach for a single-track five-layer linear wall. Each layer is linked with the discretized points at the ends as shown by the blue colour dots in Fig. 5(a). The blue dots show the deposition start and end points for a particular layer. The

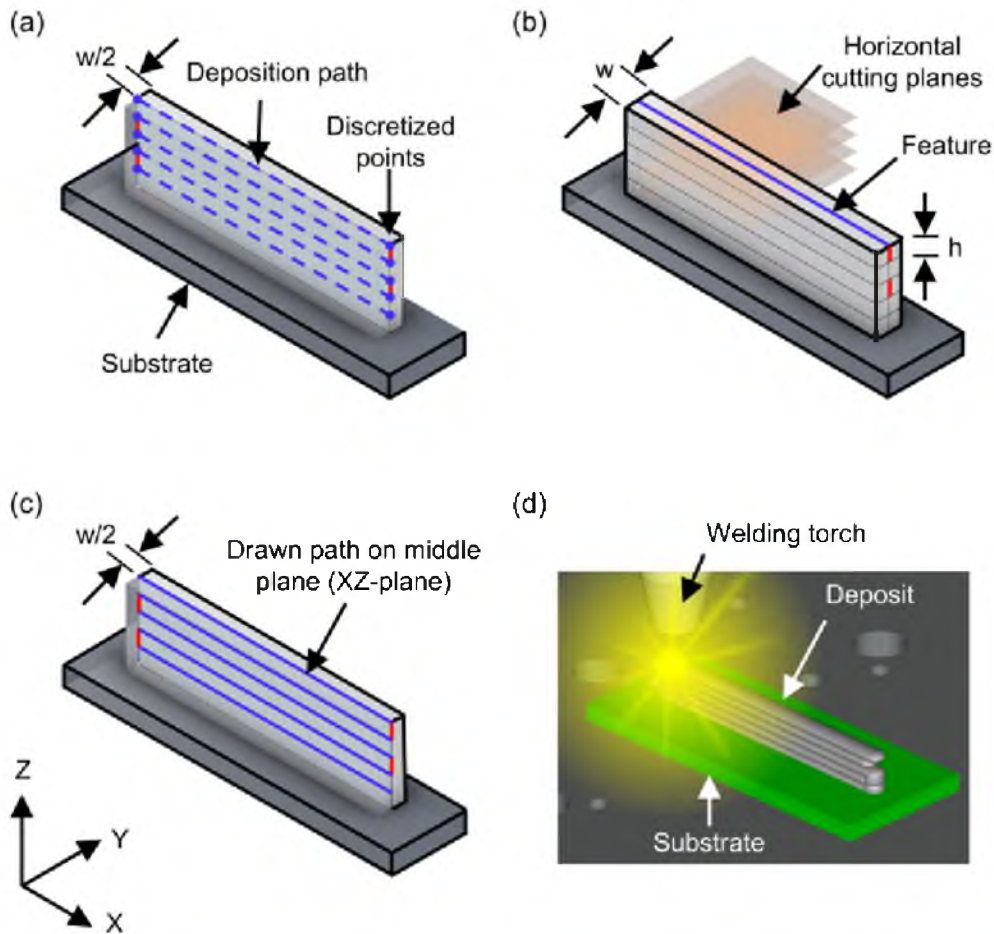


Fig. 5 : (a-c) Path generation for single-track five-layer wall deposition using (a) point-based, (b) feature-based and (c) drawing-based approaches; (d) virtual deposition simulation of linear wall. w and h are the single-track width and height, respectively.

depositing and non-depositing paths are represented by the blue dashed and red solid lines, respectively. In this bidirectional scanning strategy, a minimum of one point is necessary for every change in direction, resulting in ten discretized points for five layers as shown in **Fig. 5(a)**.

Fig. 5(b) shows the sliced CAD geometry of the single-track five-layer linear wall and the substrate, in which the deposition path is developed using feature-based approach shown by solid blue colour line at the middle. The CAD model of the wall is sliced vertically using the horizontal cutting planes (*xy*-plane) as shown in **Fig. 5(b)**. These horizontal cutting planes are at the distance of preset layer height (*h*) which is equal to the single-track height at certain WFR and PTS.

Fig. 5(c) shows the CAD geometry of the single-track five-layer linear wall and the substrate, in which the deposition path shown by blue line is developed using the drawing-based approach. A longitudinal vertical cutting plane (*xz*-plane) is positioned along the half-width (*w/2*) of the CAD geometry of the wall to facilitate the symmetry for drawing path at the middle vertical plane. The deposition path is traced from bottom to top in a layer-wise manner (**Fig. 5c**), assuming a constant layer height (*h*), which streamlines the path generation process in the robot-specific software.

Fig. 5(d) shows an image from the virtual simulation of the single-track five-layer wall deposition to validate the generated robot program before converting it into TPP. The deposition related instructions such as arc-on, arc-off and wait time need to be checked during the virtual simulation. The generated

path program is required to be modified in case of any perturbation in the scanning strategy and positional accuracy of welding torch. It is noted that the simulation time for all three approaches is approximately 30 seconds, assuming a printing travel speed of 20 mm/sec.

Table 1 presents a comparison of the performance indices for the three approaches such as the CPU time, program length, ease for program modification and software involvement. The CPU time is measured as the total time taken by software involvement, includes the Python script, CAD software, and robot-specific software on a 16-core computer. The point-based approach requires less CPU time because the scan path is automatically generated by a Python script. In contrast, it is done manually in the feature- and drawing-based approaches. Therefore, if any changes are needed in the dimensions of the CAD geometry, it is easier to regenerate the path with the point-based approach.

Overall, the point-based approach is the best for simple single-track multi-layer wall deposition. However, it is not suitable for complex irregular geometries because finding the starting point on the edge of the CAD model for the welding torch on each layer is challenging. Additionally, a huge number of discretized points are generated for the larger CAD models, which makes the manual insertion of weld instructions in robot-specific software becomes difficult and time-consuming consequently. The feature- and drawing-based methods are more practical and easier for multi-track multi-layer builds, as explained in the following section.

Table 1 : Comparison of performance indices of three CAD-to-Print approaches for single-track multi-layer linear wall deposition

Performance index	Point-based	Feature-based	Drawing-based
CPU time	17 min	23 min	25 min
Robot program length	114 lines	100 lines	100 lines
Insertion of weld related instruction	Manually added	Automatic	Automatic
Generation of path	Easier	Easy	Difficult
Regeneration of the path If any modification in the CAD geometry	Easier	Easy	Difficult
Software involvement	CAD and robot specific software, Python language for discretization	CAD and robot specific software	CAD and robot specific software

3.2. Multi-track multi-layer non-linear build

To evaluate the capabilities of the feature- and drawing-based approaches, the multi-track multi-layer non-linear build is selected for this study.

Fig. 6(a-b) show the generated robot scan paths for the multi-track multi-layer non-linear builds using a feature-based approach with different orientations of vertical cutting planes in xz- and yz-planes, respectively. The orientation of the horizontal cutting planes is same in xy-plane for slicing of the build in multiple layers as shown in Figs 6(a-b). The non-linear edge of the CAD model is assumed as the following mathematical expression of a sine curve,

$$y = A \sin \left(\frac{2\pi}{\lambda} \right) x \quad \dots\dots\dots 1$$

where, A and λ are the amplitude and wavelength of the sine curve, respectively, with the assumed values of 10 mm and 100 mm. The dimensions of the given CAD geometrical model are 100 mm (length), 10 mm (height), and 25 mm (width). As the assumed single-track height is 2 mm, the total number of layers are five to achieve the total height of 10 mm. Considering the assumed values of the single-track width as 5 mm, the hatch spacing is estimated around 3.1 mm for multi-track depositions [20]. The number of tracks vary according to the orientation of the vertical planes as shown in Fig. 6(a) and 6(b). A bidirectional scanning strategy is adopted for both tracks and layers. The depositing and non-depositing paths are illustrated by the blue and red solid lines, respectively (Fig. 6(a-b)).

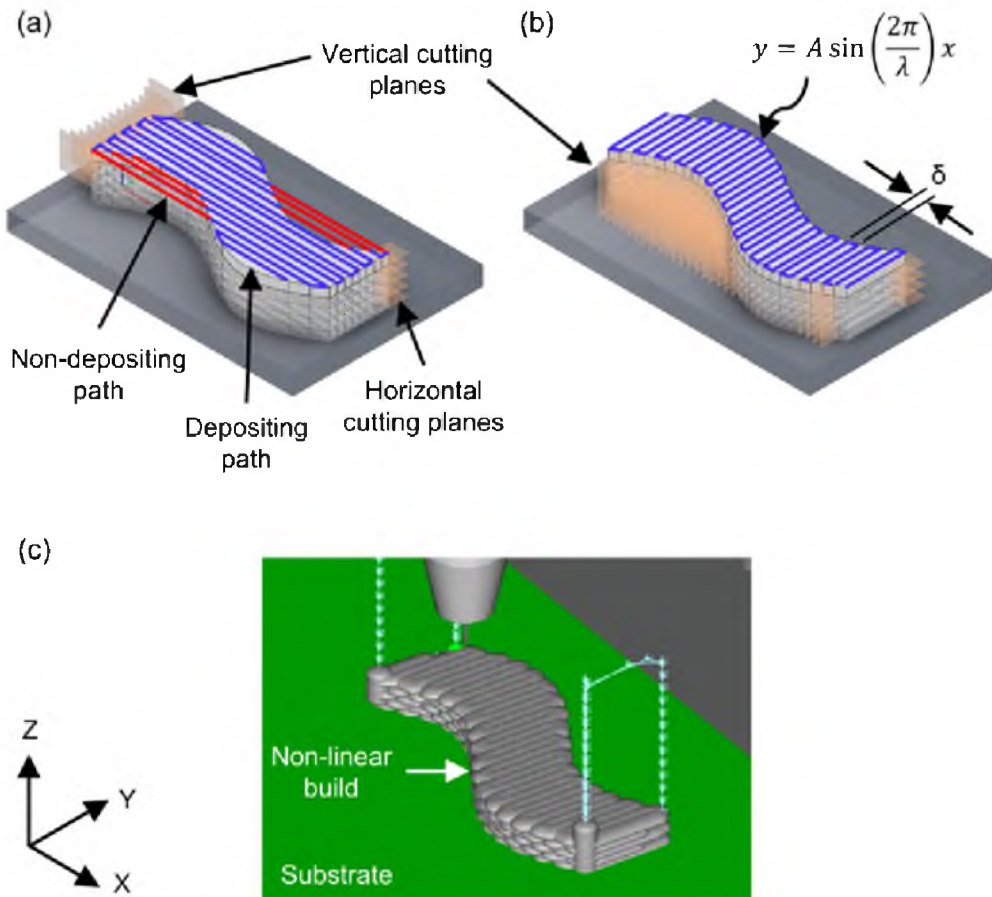


Fig. 6 : (a-b) Path generation for multi-track multi-layer non-linear build deposition using feature-based approach with different orientations of vertical cutting planes; (c) virtual deposition simulation of non-linear build using suitable feature-based approach.

Fig. 6(a) shows the scan paths developed by using feature-based approach considering the xz -planes as the vertical cutting planes. With a CAD bounding box width of 45 mm and a hatch spacing of 3.1 mm, a total of fourteen bidirectional tracks are generated utilizing thirteen cutting planes as shown in **Fig. 6(a)**. However, due to the non-linearity of the CAD model along the deposition path, the track length of 100 mm is interrupted at the curved region. This interruption results in multiple starts and stops of the welding torch during the actual deposition process leading to dimensional inconsistency, hump and crater defects [1]. To avoid these issues, alternative approaches for vertical slicing is being explored and presented further.

Fig. 6(b) shows the scanning strategy developed by using the feature-based approach considering the yz -planes as the vertical cutting planes. This configuration generates a total of thirty-two bidirectional tracks by employing thirty-one cutting planes, with each track having a length of 25 mm along y -axis (**Fig. 6(b)**). In comparison to the generated deposition path in **Fig. 6(a)**, this approach is likely to provide better dimensional consistency due to lesser number of start and end events of the welding torch as shown in **Fig. 6(b)**.

Fig. 6(c) shows the image captured from the virtual simulation of the thirty-two tracks and five layers to validate the robot program generated using the feature-based approach as

shown in **Fig. 6 (b)**. After the arc end event, the torch is uplifted to safe height of 50 mm in z -direction (**Fig. 6(c)**) to avoid any collision with the already deposited tracks / layers. Notably, the simulation time for this approach is approximately 266 seconds, assuming a printing travel speed of 20 mm/sec.

The feature-based approach encounters limitations when the torch needs to traverse along a curvilinear path. In such cases, the drawing-based approach emerges as a viable alternative. Below, the drawing-based approach tailored for multi-track multi-layer non-linear builds is presented.

Fig. 7(a) shows the scan paths generated by the drawing-based approach. With the same CAD model of dimensions 100 mm (length) x 10 mm (height) x 25 mm (width), and a hatch spacing of 3.1 mm, a total of eight bidirectional tracks are drawn on the CAD surface according to the sine curve outlined in equation (1), and shown by solid blue colour line in **Fig. 7(a)**. As a result of the change in the deposition direction, as shown in **Fig. 7(a)**, the length of a particular track equals to around 109.2 mm. A similar bidirectional scanning strategy is considered for both the tracks and layers. **Fig. 7(b)** shows the virtual simulation of eight-track five-layer non-linear build deposition, which is programmed using the drawing-based approach as shown in **Fig. 7(a)**. A better dimensional consistency probably achieved by torch path along the non-linear path and bi-directional tracks and layers.

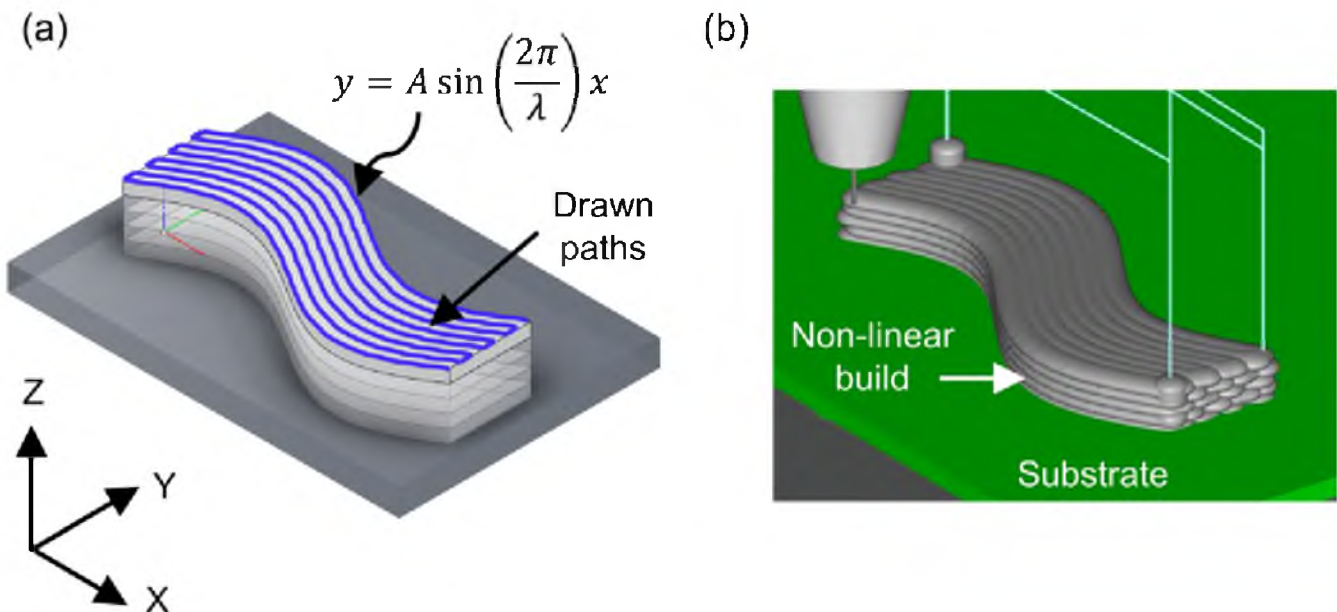


Fig. 7 : (a) Path generation for multi-track multi-layer using drawing-based approach; (b) virtual deposition simulation of non-linear build deposition.

Table 2 : Comparison of performance indices of two CAD-to-Print approaches for multi-track multi-layer non-linear build deposition

Performance index	Feature-based	Drawing-based
CPU time	350 min	400 min
Robot program length	560 lines	1215 lines
Insertion of weld related instruction	Automatic	
Generation of path	Easy	
Regeneration of the path if any modification in the CAD geometry	Easy	
Software involvement	CAD and robot specific software	

Table 2 presents a comparison of significant performance indices for the multi-track multi-layer non-linear build deposition using suitable feature- and drawing-based approach. The CPU time and program length in drawing-based approach is more as compared to the feature-based approach due to a greater number of points required along the curvilinear path.

3.3. Dimensional comparison between CAD geometry and actual deposit

To examine the efficacy of the different CAD-to-Print approaches, sample single-track multi-layer wall and multi-track multi-layer non-linear builds are deposited on a 6 mm thick AA6061 aluminium alloy substrate using a 1 mm diameter filler wire of AA5356. An advanced GMA power source (Fronius 500 TPSi) is used for preparing the sample depositions. A six-axis FANUC robot (Arc Mate 100iD/8L) with a stationary two-axis positioner is used to move the welding torch along the scan path generated using different approaches. The welding torch is kept perpendicular throughout the deposition. All

deposits are prepared at a WFR of 11 m/min, a PTS of 20 mm/s, an interpass temperature of 373 K and Ar (99.999 % purity) as a shielding gas at a flow rate of 15 l/min.

Fig. 8(a) shows the single-track five-layer wall deposit, which is compared with the CAD geometry of the deposit. Similarly, **Fig. 8(b-c)** show the multi-track five-layer deposit prepared using feature-based (**Fig. 6(c)**) and drawing-based (**Fig. 7(b)**) approaches, respectively. The length, width and height of the actually deposited wall are measured at five different locations, and the average value is considered for the comparison with the corresponding dimensions of the CAD model.

Table 3 shows the comparison between the dimensions of CAD model and actual deposit for single-track five-layer wall (**Fig. 8(a)**) and multi-track five-layer build (**Figs. 8(b-c)**). Following points are noteworthy. Firstly, the measured wall height is found lesser than the CAD height by 30%, which is attributed to the partial remelting of the previously deposited layer and flow of molten metal over its curved surface. This huge difference in the height can be mitigated by the adaptive

Table 3 : Dimensional comparison between the CAD model and the actual deposit

	Single-track Five Layer Wall			Multi-track Five Layer Wall					
	Length	Width	Height	Feature-based			Drawing-based		
Length				Width	Height	Length	Width	Height	
CAD dimension(mm)	100	5	10	100	25	10	100	25	10
Deposit dimension (mm)	105.7 (±0.3)	5.2 (±0.2)	7.0 (±0.3)	105.0 (±0.9)	27.9 (±1.1)	10.4 (±0.3)	103.5 (±0.8)	25.5 (±1.1)	12.3 (±1.2)
Deviation (%)	6	4	-30	5	11	4	4	2	23

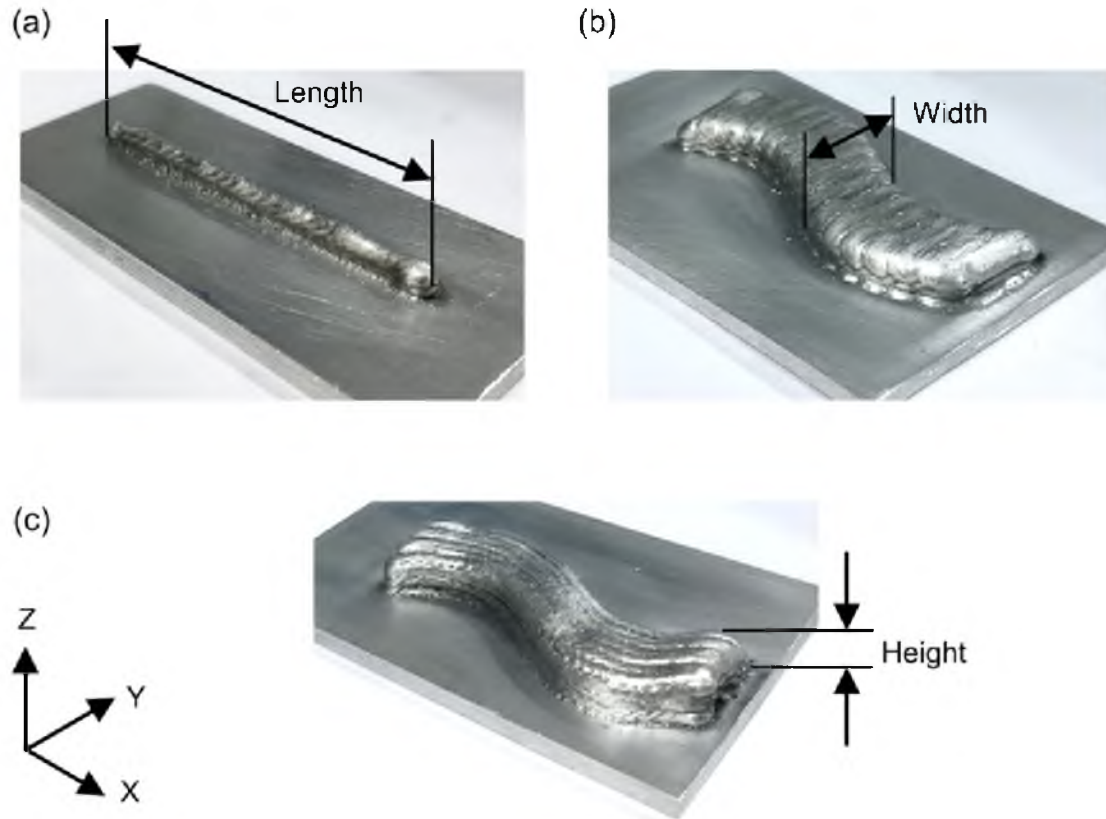


Fig. 8 : Deposited (a-c) single-track multi-layer wall and multi-track multi-layer non-linear builds shown in Fig.5(d), Fig. 6(c) and Fig. 7(b), respectively.

layer height considering the remelting of previous layer. Secondly, the feature-based approach provides lesser deviation with the CAD model in comparison with the drawing-based approach for multi-track multi-layer build. Thirdly, the multi-track multi-layer build achieves greater height than the single-track multi-layer build for the same number of layers (Table 3), which is attributed to the restricted flow of the molten metal during multi-track deposition [22].

4.0 SUMMARY AND CONCLUSIONS

In summary, three strategies are presented here for easy-to-use CAD-to-Print solution for robotic GMA-DED. The point-based approach stands out as the most efficient option for regular simple shapes, demanding minimal pre-processing time. In contrast, the feature-based approach excels for the printing of irregular shapes with linear paths. The drawing-based approach can be a substantive one for printing of parts requiring curvilinear paths. Following are the main conclusions of this work.

- Integration of a robot specific software with an open source CAD software is an effective route for effective path planning for robotic GMA-DED of a part. The same can be automated further for any complex part geometry.
- The overall percentage difference between the dimensions of CAD geometry and actual deposit are found minimum for the feature-based approach.
- A knowledge of the effect of the important process conditions such as wire feed rate, printing travel speed, hatch spacing and scanning strategy on the dimensional consistency of the deposition profile is a must for a successful CAD-to-Print operation with GMA-DED.

ACKNOWLEDGEMENT

We gratefully acknowledge the support from the Indo-German Science and Technology Centre (IGSTC) grant IGSTC/Call 2020/RAMFLICS/52/2021-22/253 for carrying out this work at the Indian Institute of Technology Bombay.

REFERENCES

- [1] Yuan L, Pan ZX, Ding DH, He FY, van Duin S, Li HJ and Li WH (2020); Investigation of humping phenomenon for the multi-directional robotic wire and arc additive manufacturing, *Robot. Comput. Integr. Manuf.*, 63, p.13.
- [2] Goswami T, Biswas S, Das S, and Mukherjee M (2022); An overview of wire arc additive manufacturing (WAAM) technique with different alloy in modern manufacturing industries. *Hybrid Metal Additive Manufacturing*, pp. 19-29.
- [3] Wang WM, van Keulen F and Wu J (2023); Fabrication sequence optimization for minimizing distortion in multi-axis additive manufacturing, *Comput. Meth. Appl. Mech. Eng.*, 406, pp.1-18.
- [4] Yuan L, Ding DH, Pan ZX, Yu ZP, Wu BT, van Duin S, Li HJ and Li WH (2020); Application of multidirectional robotic wire arc additive manufacturing process for the fabrication of complex metallic parts, *IEEE Trans. Ind. Inform.*, 16, pp.454-464.
- [5] Pan ZX, Polden J, Larkin N, Van Duin S and Norrish J (2012); Recent progress on programming methods for industrial robots, *Robot. Comput. Integr. Manuf.*, 28, pp.87-94.
- [6] Ribeiro FM, Pires JN and Azar AS (2019); Implementation of a robot control architecture for additive manufacturing applications, *Ind. Robot.*, 46, pp.73-82.
- [7] Jiang JC, Newman ST and Zhong RY (2021); A review of multiple degrees of freedom for additive manufacturing machines, *Int. J. Comput. Integr. Manuf.*, 34, pp.195-211.
- [8] Ding DH, Shen C, Pan ZX, Cuiuri D, Li HJ, Larkin N and van Duin S (2016); Towards an automated robotic arc-welding-based additive manufacturing system from CAD to finished part, *Comput. Aided Des.*, 73, pp.66-75.
- [9] Diourte A, Bugarin F, Bordreuil C and Segonds S (2021); Continuous three-dimensional path planning (CTPP) for complex thin parts with wire arc additive manufacturing, *Addit. Manuf.*, 37, pp.1-15.
- [10] Miche F, Lockett H, Ding JL, Martina F, Marinelli G and Williams S (2019); A modular path planning solution for wire plus arc additive manufacturing, *Robot. Comput. Integr. Manuf.*, 60, pp.1-11.
- [11] Giordano A, Diourte A, Bordreuil C, Bugarin F and Segonds S (2022); Thermal scalar field for continuous three-dimensional tool path strategy using wire arc additive manufacturing for free-form thin parts, *Comput. Aided Des.*, 151, p.16.
- [12] Chernovol N, Lauwers B and Rymenant PV (2020); Development of low-cost production process for prototype components based on wire and arc additive manufacturing (WAAM), *Procedia CIRP*, 95, pp.60-65.
- [13] Onstein IF, Evjemo LD and Gravdhal JT (2020); Additive manufacturing path generation for robot manipulators based on CAD models, *IFAC-Papers OnLine*, 53, pp.10037-10043.
- [14] Ding DH, Pan ZX, Cuiuri D and Li HJ (2014); A tool-path generation strategy for wire and arc additive manufacturing, *Int. J. Adv. Manuf. Technol.*, 73, pp.173-183.
- [15] Ding D, Pan Z, Cuiuri D and Li H (2015); A multi-bead overlapping model for robotic wire and arc additive manufacturing (WAAM), *Robot. Comput. Integr. Manuf.*, 31, pp.101-110.
- [16] Hao L, Mo R and Wei B (2019); CAD model segmentation algorithm using the fusion of PERT and spectral technology, *Math. Probl. Eng.*, 2019, pp.1-13.
- [17] Paul AR, Mukerjee M, Raja M, Kundu S and Chatterjee A (2022); Development of near homogeneous properties in wire arc additive manufacturing process for near-net shaped structural component of low-carbon steel. *Proceedings of the Institute of Mechanical Engineering Science*, 236(7), pp. 3497-3511.
- [18] Robot specific software: Fanuc Roboguide. <https://www.fanucamerica.com/products/robots/robot-simulation-software-FANUC-ROBOGUIDE>. Accessed on 05 February 2024.
- [19] Open source CAD software: Autodesk Fusion 360. <https://www.autodesk.com/education/edu-software/overview?sorting=featured&filters=individual>. Accessed on 05 February 2024.
- [20] Chaurasia PK, Goecke SF and De A (2023); Monitoring melt pool asymmetry in gas metal arc-directed energy deposition, *Sci. Technol. Weld. Join.*, 28, pp.424-432.
- [21] Chaurasia PK, Goecke SF and De A (2023); Towards real-time monitoring of metal transfer and melt pool temperature field in gas metal arc directed energy deposition, *Weld. World.*, 67, pp.1781-1791.
- [22] Chaurasia PK, Barik BK, Das A, Goecke SF and De A (2024); Probing dimensional consistency during multi-track multi-layer gas metal arc directed energy deposition of aluminium alloys, *Weld. World.*, 68, pp.925-938.

APPENDIX- I

Fig. I illustrates the cutting plane (P) represented by the hatched region. Point A is positioned at coordinates (x_a, y_a, z_a) , while point B lies on the plane with coordinates (x_b, y_b, z_b) . We can formulate the equation for the cutting plane perpendicular to the edge line AB, passing through point B, as expressed in the equation 1. The cutting plane in any given direction can be determined using equation 2.

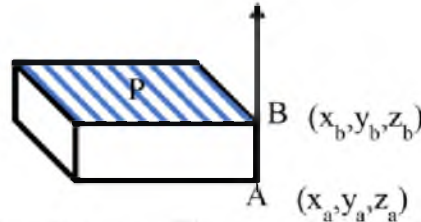


Fig. I: Illustration of cutting plane (P) perpendicular to the vector AB.

$$(x_b - x_a)(x - x_b) + (y_b - y_a)(y - y_b) + (z_b - z_a)(z - z_b) = 0 \quad (1)$$

$$P' = M_x M_y M_z P \quad (2)$$

where,

$$M_x = \begin{pmatrix} 1 & 0 & 0 \\ 0 & \cos \alpha & -\sin \alpha \\ 0 & \sin \alpha & \cos \alpha \end{pmatrix} \quad (3)$$

$$M_y = \begin{pmatrix} \cos \beta & 0 & \sin \beta \\ 0 & 1 & 0 \\ -\sin \beta & 0 & \cos \beta \end{pmatrix} \quad (4)$$

$$M_z = \begin{pmatrix} \cos \gamma & -\sin \gamma & 0 \\ \sin \gamma & \cos \gamma & 0 \\ 0 & 0 & 1 \end{pmatrix} \quad (5)$$

where, α , β , γ represent the angles of the plane with respect to the x, y, and z-axes, respectively.